DOI: 10.1002/anie.201306770

Carbon-Fiber Memory Devices

Preparation of Weavable, All-Carbon Fibers for Non-Volatile Memory Devices**

Gengzhi Sun, Juqing Liu, Lianxi Zheng, Wei Huang, and Hua Zhang**

Over the past decade, organic/polymer non-volatile memory devices with a typical configuration of organic active materials sandwiched between two electrodes have attracted increasing interest owing to their low cost, simple structure, high-throughput processing techniques. In these memory devices, the most widely used electrode materials are Al, Cu, indium-tin oxide (ITO), Pt, and p-doped or n-doped Si.[1,2] Essentially, future electronic integrates are expected to possess advanced functionalities, such as flexibility, wearability, stretchability, and transparency. Therefore, a proper substitute for rigid electrodes, such as graphene electrodes, polymer electrodes,[3–8] is required during the fabrication of memory devices. Fiber-based electronic devices, such as light emitting devices, solar cells, and photodetectors,[9–11] have exhibited mechanical reliability, flexibility, nonplanar architectures, and the possibility of integrating a large number of components in fabrics for future e-textile applications.[12–14]

Multi-walled carbon nanotube (MWCNT) fibers spun from vertically aligned arrays, which are assembled by millions of interconnected individual nanotubes, inherit the properties of individual MWCNTs and have been extensively studied in various applications.[9,11,15–22] Compared to the traditional rigid electrode materials or recently explored flexible films, MWCNT fiber-based electrodes showed some unique and promising advantages. For example, the closely packed MWCNT fibers exhibited excellent mechanical properties, they are much stronger than synthetic polymer fibers and comparable to the strongest commercial carbon fibers, leading to high mechanical reliability.[23] In addition, as the MWCNTs are highly aligned, the fiber showed excellent electrical conductivity, which makes it a promising candidate for a conducting electrode material (highly electron transport channel).[24] Moreover, the fiber is flexible, light-weight, and can be woven. Most importantly, the fiber-spinning process is compatible with conventional fiber spinning processes.[18,25,26] Recently, the MWCNT fibers have been used for various applications, such as fiber-based energy converters, chemical batteries, supercapacitors.[11,22] However, to date, there is no report on MWCNT fiber-based memory devices.

Herein, for the first time, we report a prototype of a highly efficient, weavable, fiber-based, non-volatile memory device, in which the MWCNT fiber is used as the conductive electrode material, and graphene oxide (GO) is employed as active material which is primarily coated on the outer surface of MWCNT fiber, so that a kind of core–shell structure, referred to as MWCNT@GO fiber, is obtained. By simply cross-stacking two MWCNT@GO fibers, the weavable, all-carbon fiber-based electronic device is fabricated. The memory effect of the as-fabricated device for data storage is systematically investigated.

The fabrication of weavable, MWCNT@GO fiber-based memory device is schematically shown in Figure 1. The MWCNT fibers were prepared based on our previous work (Figure 1 A; see the Experimental Section for details).[17] The thickness of the MWCNT array used for the preparation of MWCNT ribbons is approximately 400 μm and the MWCNTs are well aligned in the vertical direction (Supporting Information, Figure S1A). The average diameter of MWCNTs is approximately 13 nm (Figure S1B). Briefly, the MWCNT ribbons were directly drawn from the grown spinnable MWCNT array. By introducing twisting and densification at the same time, the wide ribbons were narrowed down and then packed into dense fibers. The twisting process resulted in the close contact between the MWCNTs and therefore enhanced the interfacial interactions among the MWCNTs. Wetting with ethanol provided further densification, leading to the small fiber diameter and a relatively smooth surface as a result of the radial contraction induced by capillary forces. The device fabrication process is shown in Figure 1 B. Briefly, a dip-coating process was employed to coat a thin layer of GO nanosheets on the surface of MWCNT fibers. Then, the resulting MWCNT@GO fibers were placed in parallel onto a substrate, on top of which another set of MWCNT@GO

[*] Dr. G. Z. Sun,[+] Prof. L. X. Zheng
School of Mechanical and Aerospace Engineering
Nanyang Technological University
50 Nanyang Avenue, Singapore 639798 (Singapore)
E-mail: lxzheng@ntu.edu.sg
Dr. J. Q. Liu,[+] Prof. H. Zhang
School of Materials Science and Engineering
Nanyang Technological University
50 Nanyang Avenue, Singapore 639798 (Singapore)
E-mail: hzhang@ntu.edu.sg
Dr. J. Q. Liu,[+] Prof. W. Huang
Singapore-Jiangsu Joint Research Center for Organic/Bio-Electronics and Information Displays & Institute of Advanced Materials (IAM), Nanjing Tech University
Nanjing 211816 (China)
[+] These authors contributed equally to this work.

[**] This work was supported by MOE under AcRF Tier 2 (ARC 10/10, No. MOE2010-T2-1-060), AcRF Tier 1 (RG 61/12), and Start-Up Grant (M4080865.070.706022) in Singapore, the "973" project (2009CB930600), NNSFC (61376088, 51302134), NSF of Jiangsu Higher Education Institutions (13KJB510012), and NSF of Jiangsu Province (BK20130934). This research is also funded by the Singapore National Research Foundation and the publication is supported under the Campus for Research Excellence And Technological Enterprise (CREATE) programme (Nanomaterials for Energy and Water Management).

Supporting information for this article is available on the WWW under http://dx.doi.org/10.1002/anie.201306770.

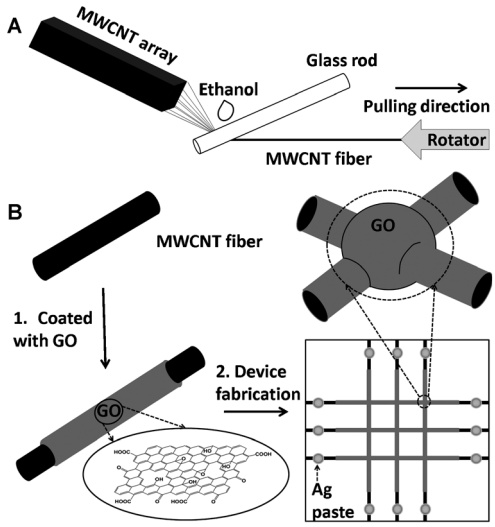

Figure 1. A) Schematic diagram of the spinning process for the formation of MWCNT fibers. B) Schematic illustration of the fabrication of the MWCNT@GO fiber-based memory device.

fibers crossed at right angles. Silver paste was used for the electrical connection. The linear relationship between voltage and current, shown in Figure S2 of the Supporting Information, indicated the Ohmic contact between the MWCNT fiber and the Ag paste,[27] which is consistent with our previous study.[28]

The morphologies of the MWCNT@GO fibers and memory devices were characterized by field emission scanning electronic microscope (SEM; Figure 2). When we use tweezers to clip a small MWCNT bundle from one side of an array, a continuous MWCNT ribbon could be pulled out.[15] The corresponding SEM image of MWCNT ribbon pulling process is shown in Figure 2 A. The inset shows the magnified SEM image of MWCNT ribbon. It can be seen that the MWCNTs are well paralleled with each other in the same orientation direction, resulting in good mechanical strength and excellent electrical conductivity of the obtained MWCNT fibers. Figure 2 B shows SEM image of a portion of the MWCNT fiber. By combining the pulling and twisting processes, the MWCNT fiber shrank and became densely packed with a small surface twist angle of 10° after it passed through ethanol. The obtained MWCNT fiber exhibits a uniform shape and a smooth surface with a diameter of around 4 μm.

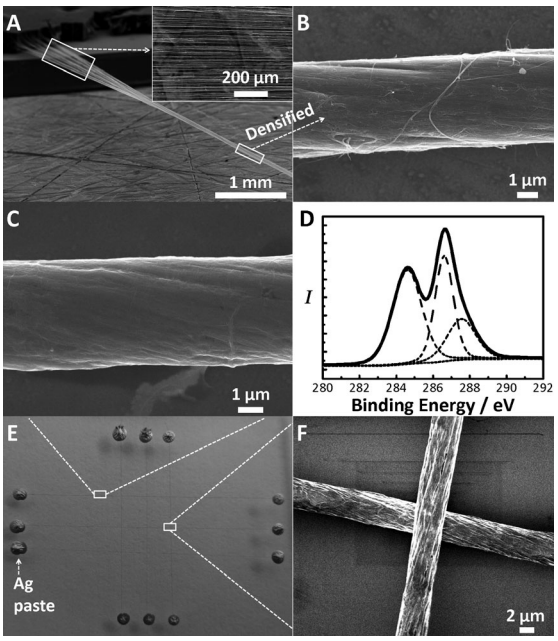

Figure 2. SEM images of A) a MWCNT ribbon pulled from a vertically aligned MWCNT array (Inset: magnified SEM image of the MWCNT ribbon), B) a MWCNT fiber, C) a MWCNT@GO fiber. D) The C 1s XPS spectrum of the GO nanosheets. E) Photograph of the fabricated MWCNT@GO fiber-based memory devices. F) SEM image of MWCNT@GO fibers at the cross area.

GO nanosheets can wrap MWCNTs in aqueous media through noncovalent interactions.[29] Thus the as-spun MWCNT fibers were first coated by a thin layer of GO nanosheets. Owing to its large lateral area, the GO nanosheets could cover a large amount of MWCNTs in the fiber. Figure 2 C shows a SEM image of a MWCNT@GO fiber. The coated GO layer, with thickness of 10–20 nm on the as-fabricated fiber cell, was characterized by SEM (Figure S3). The GO nanosheets, which were drop-casted on a cleaned Si/SiO_2 wafer, were further characterized by X-ray photoelectron spectroscopy (XPS) as shown in Figure 2 D. Three typical peaks between 282 and 290 eV could be assigned to C=C at 284.6 eV, C–O at 286.6 eV, and C=O at 287.6 eV, respectively.[30] The atomic ratio between elements of C and O is 1.89, indicating the existence of large number of oxygen-containing groups.

Based on their good flexibility and electrical properties, as a proof of concept, MWCNT fibers as conductive materials and GO as active material were used for the fabrication of electronic devices for data-storage applications. A MWCNT@GO fiber-based memory cell was realized by cross-stacking two MWCNT@GO fibers (Figure 1 B). The photograph of fabricated 3×3 devices is shown in Figure 2 E. SEM was further utilized to confirm the contact between two MWCNT@GO fibers (Figure 2 F). Moreover, the cross-sectional SEM image (Figure S4) also indicated that MWCNT@GO fibers were in good contact with each other. After the Ag paste was applied at the end of MWCNT fibers, the as-fabricated devices (Figure 2 E) were ready for electrical characterization.

Figure 3 A shows the typical memory characteristics of the MWCNT@GO fiber-based cells, where the arrows represent the sweeping direction of voltage. Initially, as a positive voltage swept from 0 to 3.5 V, the MWCNT@GO fiber cell was in a high resistance state (OFF state), and the current increased progressively with the voltage increase (stage I). When the applied voltage exceeded the switching threshold voltage of 3.5 V, an abrupt current increase occurred from 4.2×10^{-8} to 3.8×10^{-6} A (stage II), indicating a transition from the high resistance state to the low resistance state (ON state). The transition from the OFF state to the ON state is equivalent to a set/write process in a digital storage device, with a high ON/OFF current ratio of approximately 10^3:1 which is comparable with the value of GO-based memory diode using metal electrodes.[31,32] Impressively, the

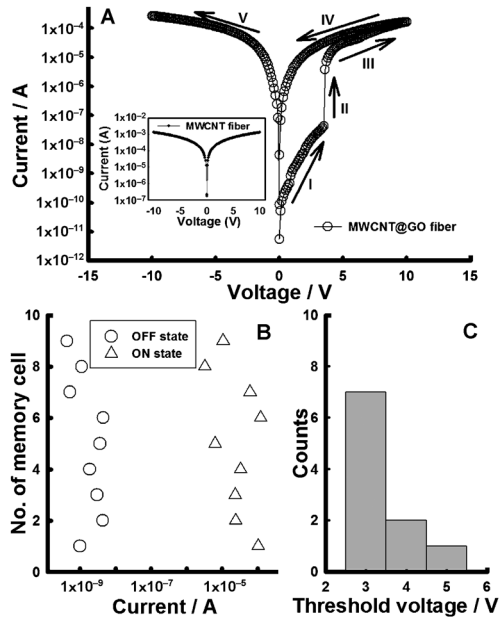

Figure 3. A) The *I–V* characteristics of the MWCNT@GO fiber-based memory cell (for arrows I–V, see text). Inset: *I–V* characteristic of MWCNT fiber-based cell. Statistical distribution of B) the ON-/OFF-state currents, C) the threshold voltages of the operative MWCNT@GO fiber-based memory cells.

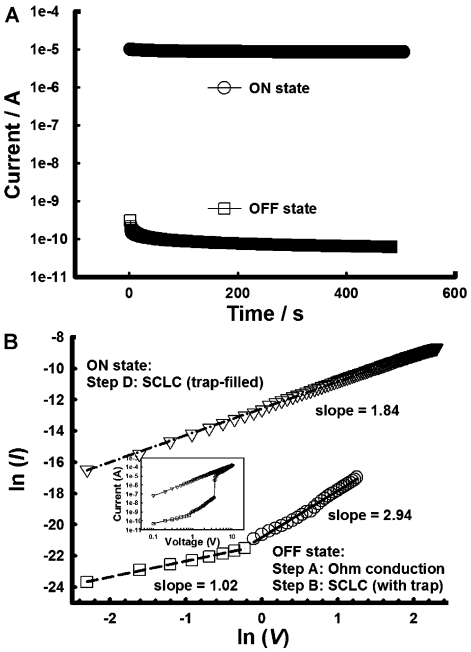

Figure 4. A) The retention-ability test of the fiber-based memory cell at a reading voltage of 1 V in the ON and OFF states. B) Experimental data and fitted lines of the *I–V* characteristics in the OFF state and ON state, (Inset: plot of the absolute value of the current as a function of applied voltage for the WORM memory cell in the positive sweep in Figure 3 A).

MWCNT@GO fiber cell retained this low resistance state in the following voltage sweeps (stage III and IV), even if the power was turned off, indicating a non-volatile behavior of the memory cell. Most importantly, the low resistance state was not retrievable by applying a reverse voltage scan (stage V), indicating that the fiber-based cell exhibits the write-once-read-many-times (WORM) type memory effect. Note that the role of coated GO layer is very important in the fabricated MWCNT@GO fiber-based memory cell. Without GO, the *I–V* curves did not exhibit the electrical switching behavior, and the memory effects was not observed (inset of Figure 3 A). The basic parameters of importance to the performance of a memory device include switching voltage, ON/OFF current ratio, and retention ability. Figure 3 B and C show the statistical distribution of the ON-/OFF-state currents (measured at 1 V) and the switching threshold voltages of the operative memory cells, respectively. The transition from the OFF state to the ON state occurred at voltages between 3.0 and 4.5 V, and these low switching voltages reveal a low writing voltage, suggesting a promising application in low power consumption memory devices. The distribution of the OFF- and ON-state current values lay within two order of magnitude, with a minimum ON/OFF current ratio of 10^2–10^3:1. The high ON/OFF current ratio promises a low misreading probability during the device operation.

To study the data-retention ability, the current–time characteristics of the ON and OFF states were investigated at a reading voltage of 1 V. As shown in Figure 4 A, the OFF and ON states remained at the same order of magnitude and did not exhibit any serious electrical degradation for 500 s. The ON/OFF current ratio stayed at over four orders of magnitude. The excellent electrical stability indicates potential applications in non-volatile memory devices. To understand the memory behavior and the carrier transport mechanism of the fiber cells, the experimental *I–V* data were fitted using different conduction models. Figure 4 b shows four major regions in the *I–V* curves, where the initial OFF state can be divided into two distinct regions, suggesting two different conduction mechanisms in the OFF state. At the voltage below 0.8 V in the initial OFF state, the *I–V* curves exhibited a linear Ohmic behavior with a slope of 1.02, which is consistent with the literature values.[32,33] As the voltage exceeding 0.8 V, the fitting line has a slope of 2.94 (greater than 2), thus trap-limited space-charge-limited-current (SCLC) dominates the carrier transport process,[34] with charge trapping on the surface defects and structural disorder of GO induced by oxidation.[35,36] With a further increase of the bias, the oxygen migration in the GO coating layer could generate resistive switching of the MWCNT@GO fiber-based cell.[31] Moreover, the injected carriers will fill all the traps in the GO coating, resulting in the trap-filled SCLC mechanism in the ON state,[37] with a slope of 1.84 (nearly equal to 2). As for the erase function of the memory devices with GO as the active material, this strongly depends on the electrode materials. The erase behavior cannot be obtained when the inert electrodes are used, such as Au or graphene.[3,31,38] In our current MWCNT@GO fiber-based memory cell, the non-erasing behavior might arise from the irreversible migration of oxygen in the GO layer owing to the relatively inert MWCNT fiber electrodes.

In summary, we have fabricated weavable, all-carbon, fiber-based memory cells consisting of GO-coated MWCNT

fibers and systematically studied their memory effect. The MWCNT fiber that was spun from vertically aligned arrays served as top and bottom electrodes. The coated GO nanosheets were used as the active layer. The prepared MWCNT@GO fiber-based device showed electrical bistability and a WORM memory effect with a minimum ON/OFF ratio of 10^3:1. Moreover, the as-prepared memory devices exhibited high reliability with a long life time in the retention test and excellent stability. The novel MWCNT@GO fiber-based structure and facile fabrication process make these memory devices promising for future smart e-textile applications.

Experimental Section

The detailed multi-walled carbon nanotube (MWCNT) growth and fiber spinning process can be found in our previous reports.[28,39,40] The spinnable vertically aligned MWCNT array was prepared by chemical vapor deposition (CVD) in a furnace equipped with a 1 inch-diameter quartz tube. Ar and C_2H_4 were used as the carrier gas and carbon source, respectively. The catalyst used was a thin-layer Fe film with a thickness of 1 nm, deposited on a Si/SiO_2 substrate by sputtering. Normally, the growth of MWCNT array was carried out under 155 sccm Ar and 45 sccm C_2H_4 at 750 °C for 10 min. The MWCNT fibers were spun from the as-prepared MWCNT array with a micro spindle mounted on a motor. During the spinning process, ethanol was applied to densify the fiber to achieve a smoother surface.

Graphene oxide (GO) was prepared by a modified Hummers method.[41] The as-prepared GO nanosheet powder was re-dispersed in water by strong ultrasonication. The obtained GO solution was centrifuged at 3000 rpm to remove the aggregates or small particles. Then the MWCNT fibers were immersed into the well-dispersed GO methanol solution (0.2 mg mL^{-1}) for ca. 2 h.[42] The GO layer coated on the MWCNT fibers was dried under ambient conditions. The procedure for coating GO layer was repeated one more time to guarantee a good coating quality. Finally, the fabricated devices were ready for the electrical tests.

The scanning electron microscopy (SEM) was recorded by using a field-emission scanning electron microscope (JEOL, Model JBM-6340F). X-ray photoelectron spectroscopy (XPS) measurements were carried out with Al Kα radiation, 1486.7 eV. The spectra were corrected by referencing the binding energy to the C1s peak at 284.6 eV. The *I–V* measurements were performed by using a Keithley 4200 semiconductor parameter analyzer under ambient conditions.

Received: August 2, 2013
Revised: September 21, 2013
Published online: November 5, 2013

Keywords: carbon nanotubes · electronics · fiber · graphene oxide · memory devices

[1] S. Möller, C. Perlov, W. Jackson, C. Taussig, S. R. Forrest, *Nature* **2003**, *426*, 166 – 169.
[2] Q. D. Ling, D. J. Liaw, C. X. Zhu, D. S. H. Chan, E. T. Kang, K. G. Neoh, *Prog. Polym. Sci.* **2008**, *33*, 917 – 978.
[3] J. Q. Liu, Z. Y. Yin, X. H. Cao, F. Zhao, L. H. Wang, W. Huang, H. Zhang, *Adv. Mater.* **2013**, *25*, 233 – 238.
[4] J. Q. Liu, Z. Q. Lin, T. J. Liu, Z. Y. Yin, X. Z. Zhou, S. F. Chen, L. H. Xie, F. Boey, H. Zhang, W. Huang, *Small* **2010**, *6*, 1536 – 1542.
[5] M. A. Khan, U. S. Bhansali, D. Cha, H. N. Alshareef, *Adv. Funct. Mater.* **2013**, *23*, 2145 – 2152.
[6] Y. S. Chen, Y. F. Xu, K. Zhao, X. J. Wan, J. C. Deng, W. B. Yan, *Nano Res.* **2010**, *3*, 714 – 721.
[7] L. Huang, Y. Huang, J. J. Liang, X. J. Wan, Y. S. Chen, *Nano Res.* **2011**, *4*, 675 – 684.
[8] J. J. Liang, Y. S. Chen, Y. F. Xu, Z. B. Liu, L. Zhang, X. Zhao, X. L. Zhang, J. G. Tian, Y. Huang, Y. F. Ma, F. F. Li, *ACS Appl. Mater. Interfaces* **2010**, *2*, 3310 – 3317.
[9] T. Chen, S. T. Wang, Z. B. Yang, Q. Y. Feng, X. M. Sun, L. Li, Z. S. Wang, H. S. Peng, *Angew. Chem.* **2011**, *123*, 1855 – 1859; *Angew. Chem. Int. Ed.* **2011**, *50*, 1815 – 1819.
[10] M. Zhang, S. L. Fang, A. A. Zakhidov, S. B. Lee, A. E. Aliev, C. D. Williams, K. R. Atkinson, R. H. Baughman, *Science* **2005**, *309*, 1215 – 1219.
[11] X. M. Sun, T. Chen, Z. B. Yang, H. S. Peng, *Acc. Chem. Res.* **2013**, *46*, 539 – 549.
[12] E. Westerweele, P. Smith, A. J. Heeger, *Adv. Mater.* **1995**, *7*, 788 – 790.
[13] M. Hamedi, R. Forchheimer, O. Inganas, *Nat. Mater.* **2007**, *6*, 357 – 362.
[14] M. Hamedi, L. Herlogsson, X. Crispin, R. Marcilla, M. Berggren, O. Inganas, *Adv. Mater.* **2009**, *21*, 573 – 577.
[15] G. Z. Sun, L. X. Zheng, J. Y. Zhou, Y. N. Zhang, Z. Y. Zhan, J. H. L. Pang, *Int. J. Plasticity* **2013**, *40*, 56 – 64.
[16] Y. N. Zhang, L. X. Zheng, G. Z. Sun, Z. Y. Zhan, K. Liao, *Carbon* **2012**, *50*, 2887 – 2893.
[17] L. X. Zheng, G. Z. Sun, Z. Y. Zhan, *Small* **2010**, *6*, 132 – 137.
[18] H. S. Peng, X. M. Sun, F. J. Cai, X. L. Chen, Y. C. Zhu, G. P. Liao, D. Y. Chen, Q. W. Li, Y. F. Lu, Y. T. Zhu, Q. X. Jia, *Nat. Nanotechnol.* **2009**, *4*, 738 – 741.
[19] G. Z. Sun, J. Y. Zhou, F. Yu, Y. N. Zhang, J. H. L. Pang, L. X. Zheng, *J. Solid State Electrochem.* **2012**, *16*, 1775 – 1780.
[20] T. Chen, L. B. Qiu, Z. B. Yang, Z. B. Cai, J. Ren, H. P. Li, H. J. Lin, X. M. Sun, H. S. Peng, *Angew. Chem.* **2012**, *124*, 12143 – 12146; *Angew. Chem. Int. Ed.* **2012**, *51*, 11977 – 11980.
[21] K. L. Jiang, J. P. Wang, Q. Q. Li, L. A. Liu, C. H. Liu, S. S. Fan, *Adv. Mater.* **2011**, *23*, 1154 – 1161.
[22] J. Ren, L. Li, C. Chen, X. L. Chen, Z. B. Cai, L. B. Qiu, Y. G. Wang, X. R. Zhu, H. S. Peng, *Adv. Mater.* **2013**, *25*, 1155 – 1159.
[23] X. F. Zhang, Q. W. Li, T. G. Holesinger, P. N. Arendt, J. Y. Huang, P. D. Kirven, T. G. Clapp, R. F. DePaula, X. Z. Liao, Y. H. Zhao, L. X. Zheng, D. E. Peterson, Y. T. Zhu, *Adv. Mater.* **2007**, *19*, 4198 – 4201.
[24] Q. W. Li, Y. Li, X. F. Zhang, S. B. Chikkannanavar, Y. H. Zhao, A. M. Dangelewicz, L. X. Zheng, S. K. Doorn, Q. X. Jia, D. E. Peterson, P. N. Arendt, Y. T. Zhu, *Adv. Mater.* **2007**, *19*, 3358 – 3363.
[25] M. Zhang, K. R. Atkinson, R. H. Baughman, *Science* **2004**, *306*, 1358 – 1361.
[26] M. D. Lima, S. L. Fang, X. Lepro, C. Lewis, R. Ovalle-Robles, J. Carretero-Gonzalez, E. Castillo-Martinez, M. E. Kozlov, J. Y. Oh, N. Rawat, C. S. Haines, M. H. Haque, V. Aare, S. Stoughton, A. A. Zakhidov, R. H. Baughman, *Science* **2011**, *331*, 51 – 55.
[27] S. M. Sze, *Physics of semiconductor devices*, Wiley, New York, **1981**.
[28] G. Z. Sun, Y. X. Huang, L. X. Zheng, Z. Y. Zhan, Y. N. Zhang, J. H. L. Pang, T. Wu, P. Chen, *Nanoscale* **2011**, *3*, 4854 – 4858.
[29] Y. Q. Li, T. Y. Yang, T. Yu, L. X. Zheng, K. Liao, *J. Mater. Chem.* **2011**, *21*, 10844 – 10851.
[30] Y. W. Zhu, M. D. Stoller, W. W. Cai, A. Velamakanni, R. D. Piner, D. Chen, R. S. Ruoff, *ACS Nano* **2010**, *4*, 1227 – 1233.
[31] H. Y. Jeong, J. Y. Kim, J. W. Kim, J. O. Hwang, J. E. Kim, J. Y. Lee, T. H. Yoon, B. J. Cho, S. O. Kim, R. S. Ruoff, S. Y. Choi, *Nano Lett.* **2010**, *10*, 4381 – 4386.
[32] F. Zhuge, B. L. Hu, C. L. He, X. F. Zhou, Z. P. Liu, R. W. Li, *Carbon* **2011**, *49*, 3796 – 3802.

[33] L. H. Wang, W. Yang, Q. Q. Sun, P. Zhou, H. L. Lu, S. J. Ding, D. W. Zhang, *Appl. Phys. Lett.* **2012**, *100*, 063509.
[34] A. Sleiman, M. F. Mabrook, R. R. Nejm, A. Ayesh, A. Al Ghaferi, M. C. Petty, D. A. Zeze, *J. Appl. Phys.* **2012**, *112*, 024509.
[35] D. Joung, A. Chunder, L. Zhai, S. I. Khondaker, *Appl. Phys. Lett.* **2010**, *97*, 093105.
[36] A. Bagri, C. Mattevi, M. Acik, Y. J. Chabal, M. Chhowalla, V. B. Shenoy, *Nat. Chem.* **2010**, *2*, 581 – 587.
[37] H. T. Lin, Z. Pei, Y. J. Chan, *IEEE Electron Device Lett.* **2007**, *28*, 569 – 571.
[38] F. Zhao, J. Q. Liu, X. Huang, X. Zou, G. Lu, P. J. Sun, S. X. Wu, W. Ai, M. D. Yi, X. Y. Qi, L. H. Xie, J. L. Wang, H. Zhang, W. Huang, *ACS Nano* **2012**, *6*, 3027 – 3033.
[39] G. Z. Sun, L. X. Zheng, J. An, Y. Z. Pan, J. Y. Zhou, Z. Y. Zhan, J. H. L. Pang, C. K. Chua, K. F. Leong, L. Li, *Nanoscale* **2013**, *5*, 2870 – 2874.
[40] G. Z. Sun, Y. N. Zhang, L. X. Zheng, *J. Nanomater.* **2012**, *2012*, 506209.
[41] G. Z. Sun, Y. Z. Pan, Z. Y. Zhan, L. X. Zheng, J. Y. Lu, J. H. L. Pang, L. Li, W. M. Huang, *J. Phys. Chem. C* **2011**, *115*, 23741 – 23744.
[42] J. Q. Liu, Z. Y. Yin, X. H. Cao, F. Zhao, A. P. Lin, L. H. Xie, Q. L. Fan, F. Boey, H. Zhang, W. Huang, *ACS Nano* **2010**, *4*, 3987 – 3992.

